In Situ Electrochemical Imaging of Membrane Glycan Expression on Micropatterned Adherent Single Cells

ARTICLE *in* ANALYTICAL CHEMISTRY · SEPTEMBER 2010

Impact Factor: 5.64 · DOI: 10.1021/ac101688p · Source: PubMed

5 AUTHORS, INCLUDING:

Yadong Xue

11 PUBLICATIONS **374** CITATIONS

SEE PROFILE

Huangxian Ju

Nanjing University

378 PUBLICATIONS **14,328** CITATIONS

SEE PROFILE

Anal. Chem. **2010,** *82,* 7112–7118

In Situ Electrochemical Imaging of Membrane Glycan Expression on Micropatterned Adherent Single Cells

Yadong Xue,[†] Lin Ding,[†] Jianping Lei,[†] Feng Yan,[‡] and Huangxian Ju*,[†]

Key Laboratory of Analytical Chemistry for Life Science (Ministry of Education of China), Department of Chemistry, Nanjing University, Nanjing 210093, P. R. China, and Jiangsu Institute of Cancer Prevention and Cure, Nanjing 210009, P. R. China

A scanning electrochemical microscopic (SECM) method for in situ imaging of four types of membrane glycan motifs on single adherent cells was proposed using BGC-823 human gastric carcinoma (BGC) cells as the model. These adherent cells were first micropatterned in the microwell of poly(dimethylsiloxane) membrane for precisely controlling the localized surface interaction, and the membrane glycans were then specifically recognized with corresponding lectins labeled with horseradish peroxidase (HRP). On the basis of the enzymatic oxidization of ferrocenylmethanol (FMA) by H_2O_2 to yield FMA^+, the glycan expression level was detected by the reduction current of FMA^+ at the SECM tip. The cell-surface glycans could, thus, be in situ imaged by SECM at a single-cell level without peeling the cells from culture dish. Under the optimized conditions, four types of membrane glycan motifs showed statistically distinguishable expression levels. The SECM results for different glycan motifs on adherent single cells were consistent with those estimated by flow cytometric assay. This work provides a reliable approach for in situ evaluation of the characteristic glycopattern of single living cells and can be applied in cell biologic study based on cell surface carbohydrate expression.

Cell-surface glycans are emerging as significant factors in cell−cell communication,[1,2] immune recognition/response,[3−6] cell adhesion, and many developmental processes.[7−10] For example, *N*-glycans of glycoproteins are frequently involved in many important biological events including protein folding, endoplasmic reticulum-associate protein degradation, cell differentiation, host−pathogen interaction, cancer metastasis, and autoimmunity.[11−13] Abnormal expression of *O*-glycans and mucins either as transmembrane proteins on the cell surface or as secreted proteins in most tumors commonly correlates with adhesion and invasion.[14,15] A growing body of evidence indicates that glycan expression alteration is a crucial hallmark of disease states at various pathophysiological steps of tumor progression.[16] Thus, highly sensitive, quantitatively accurate, and informative analytical methods and instrumentation are keenly desirable for the identification of glycan expression on cell surfaces.

Current efforts for detecting membrane glycans of cells have been focused on mass spectrometric (MS) methods.[17−19] MS techniques, combined with various glycan release and enrichment strategies, can categorize the glycome and provide molecular details. However, it is time-consuming and not amenable to living cell interrogation due to its destructive nature. Recent advances in lectin microarray technology, based on the investigation of the cell-capturing extent of different lectins, have offered exciting opportunities to unveil the mysteries of glycans in various cellular processes and disease states,[20−24] but the issues of active-site accessibility and lectin denaturation in the surface immobilization format with high density usually impair the sensitivity and stability of this technology.[25] Several electrochemical methods using lectin-based probe or lectin-modified electrode have been developed

* Corresponding author. Phone/Fax: +86-25-83593593. E-mail: hxju@nju.edu.cn.

[†] Nanjing University.

[‡] Jiangsu Institute of Cancer Prevention and Cure.

(1) Collins, B. E.; Paulson, J. C. *Curr. Opin. Chem. Biol.* **2004**, *8*, 617–625.
(2) Crocker, P. R. *Curr. Opin. Struct. Biol.* **2002**, *12*, 609–615.
(3) Kinjo, Y.; Wu, D.; Kim, G.; Xing, G.-W.; Poles, M. A.; Ho, D. D.; Tsuji, M.; Kawahara, K.; Wong, C.-H.; Kronenberg, M. *Nature* **2005**, *434*, 520–525.
(4) Rudd, P. M.; Elliott, T.; Cresswell, P.; Wilson, I. A.; Dwek, R. A. *Science* **2001**, *291*, 2370–2376.
(5) Rudd, P. M.; Wormald, M. R.; Dwek, R. A. *Trends Biotechnol.* **2004**, *22*, 524–530.
(6) Crocker, P. R. *Curr. Opin. Pharmacol.* **2005**, *5*, 431–437.
(7) Haltiwanger, R. S.; Lowe, J. B. *Annu. Rev. Biochem.* **2004**, *73*, 491–537.
(8) Hwang, H.-Y.; Olson, S. K.; Esko, J. D.; Horvitz, H. R. *Nature* **2003**, *423*, 439–443.
(9) Cipollo, J. F.; Awad, A. M.; Costello, C. E.; Hirschberg, C. B. *J. Biol. Chem.* **2005**, *280*, 26063–26072.
(10) Raman, R.; Raguram, S.; Venkataraman, G.; Paulson, J. C.; Sasisekharan, R. *Nat. Methods* **2005**, *2*, 817–824.
(11) Gamblin, D. P.; Scanlan, E. M.; Davis, B. G. *Chem. Rev.* **2009**, *109*, 131–163.
(12) Arnold, J. N.; Wormald, M. R.; Sim, R. B.; Rudd, P. M.; Dwek, R. A. *Annu. Rev. Immunol.* **2007**, *25*, 21–50.
(13) Helenius, A.; Aebi, M. *Science* **2001**, *291*, 2364–2369.
(14) Hollingsworth, M. A.; Swanson, B. J. *Nat. Rev. Cancer* **2004**, *4*, 45–60.
(15) Bharathan, S.; Moriarty, J.; Moody, C. E.; Sherblom, A. P. *Cancer Res.* **1990**, *50*, 5250–5256.
(16) Fuster, M. M.; Esko, J. D. *Nat. Rev. Cancer* **2005**, *5*, 526–542.
(17) Kameyama, A.; Kikuchi, N.; Nakaya, S.; Ito, H.; Sato, T.; Shikanai, T.; Takahashi, Y.; Takahashi, K.; Narimatsu, H. *Anal. Chem.* **2005**, *77*, 4719–4725.
(18) Liu, X.; McNally, D. J.; Nothaft, H.; Szymanski, C. M.; Brisson, J.-R.; Li, J. *Anal. Chem.* **2006**, *78*, 6081–6087.
(19) Goetz, J. A.; Novotny, M. V.; Mechref, Y. *Anal. Chem.* **2009**, *81*, 9546–9552.

10.1021/ac101688p
Published on Web 08/04/2010

for the sensitive evaluation of surface glycans and monitoring of dynamic changes in the glycosylation status.[25−28] However, these methods only offer the information of the average expression level of a cell population and, thus, possibly enshroud the heterogeneity of single cells, which might be indicative of disease in the early stage.[29] Moreover, these methods are applicable for cell suspension, obtained by peeling cells from the culture dish, leading to unexpected changes in the state of cell surface.[30,31] Similar issue also exists in flow cytometry for estimating the glycan expression level.[32] Thus, a noninvasive and sensitive method at single-cell level is urgently required for in situ detection of membrane glycans on adherent cells. Most trusted data by the cell biology community is collected on adherent cells, and the ability to study single cells in the adherent state is exciting.

Scanning electrochemical microscopy (SECM) is a scanning probe technique, by which the localized chemical reaction under near physiological conditions can be quantitatively monitored in a noninvasive manner. Therefore, it has been successfully used to in situ study both biological systems and physiological processes at single-cell level, such as measuring enzymatic activity,[33−36] monitoring the cellular metabolism,[37−39] investigating the neurotransmitter secretion,[40,41] and imaging the topography.[42−44] Most recently, the membrane protein imaging of single living cells with SECM has been proposed using alkaline phosphatase-labeled antibodies and detecting the oxidation current of the enzymatic product, *p*-aminophenol, at an electrode with the Pt-disk diameter of 20 μm.[45] Here, a SECM method for in situ electrochemical imaging of different surface glycan motifs on adherent cells at the single-cell level was presented using horseradish peroxidase (HRP)-tagged lectins coupled with micropatterning (Figure 1).

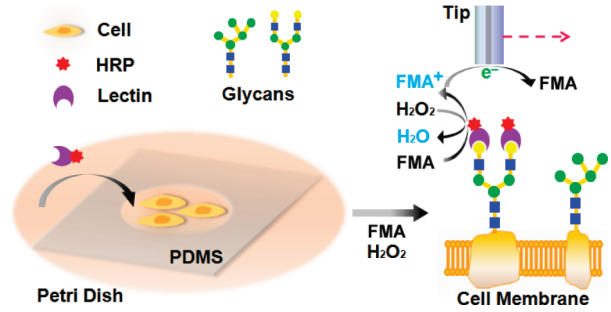

Figure 1. Scheme of SECM imaging for cell-surface glycan expression using SG/TC mode.

The practicality of the SECM method for in situ detection of membrane glycans on adherent cells was verified using BGC-823 human gastric carcinoma (BGC) cells as the model. The localized surface interaction on the cell surface was precisely controlled by a poly(dimethylsiloxane) (PDMS) membrane with handmade microwells. The HRP-tagged lectins could specifically bind to membrane glycans to catalyze the oxidation of ferrocenylmethanol (FMA) by H_2O_2 to FMA^+.[46,47] Using a substrate generation/tip collection (SG/TC) mode, the generated FMA^+ diffused to the tip of a scanning 2 μm Pt-disk probe set at 0.05 V (vs Ag/AgCl) to produce the reduction current for imaging the expression level of membrane glycans. This work afforded a noninvasive strategy for detecting membrane glycans of single cells. This strategy could be potentially applied to in situ monitoring of dynamic changes in the glycosylation status on adherent cell surfaces and had promising application in cell biologic study based on cell-surface carbohydrate expression.

EXPERIMENTAL SECTION

Materials and Reagents. HRP-tagged concanavalin A (HRP-ConA), HRP-tagged wheat germ agglutinin (HRP-WGA), HRP-tagged *Dolichos biflorus* agglutinin (HRP-DBA), HRP-tagged peanut agglutinin (HRP-PNA), bovine serum albumin (BSA), and FMA were purchased from Sigma-Aldrich Inc. (USA). Fluorescein lectin kit I containing fluorescein isothiocyanate (FITC)-labeled lectins (DBA, ConA, PNA, and WGA) was purchased from Vector laboratories Inc. (USA). Sylgard 184 silicone elastomer and curing agent were purchased from Dow Corning (Midland, MI). Phosphate-buffered saline (PBS, pH 7.4) containing 136.7 mM NaCl, 2.7 mM KCl, 87 mM Na_2HPO_4, and 14 mM KH_2PO_4 was sterilized before use. All aqueous solutions were prepared using ≥18 MΩ ultrapure water purified with a Millipore Milli-Q system.

(20) Lis, H.; Sharon, N. *Chem. Rev.* **1998**, *98*, 637–674.
(21) Zheng, T.; Peelen, D.; Smith, L. M. *J. Am. Chem. Soc.* **2005**, *127*, 9982–9983.
(22) Hsu, K.; Pilobello, K. T.; Mahal, L. K. *Nat. Chem. Biol.* **2006**, *2*, 153–157.
(23) Tateno, H.; Uchiyama, N.; Kuno, A.; Togayachi, A.; Sato, T.; Narimatsu, H.; Hirabayashi, J. *Glycobiolgy* **2007**, *17*, 1138–1146.
(24) Huang, W.; Wang, D.; Yamada, M.; Wang, L. X. *J. Am. Chem. Soc.* **2009**, *131*, 17963–17971.
(25) Ding, L.; Cheng, W.; Wang, X.; Ding, S.; Ju, H. X. *J. Am. Chem. Soc.* **2008**, *130*, 7224–7225.
(26) Cheng, W.; Ding, L.; Lei, J.; Ding, S.; Ju, H. X. *Anal. Chem.* **2008**, *80*, 3867–3872.
(27) Cheng, W.; Ding, L.; Ding, S.; Yin, Y.; Ju, H. X. *Angew. Chem., Int. Ed.* **2009**, *48*, 6465–6468.
(28) Ding, L.; Cheng, W.; Wang, X.; Xue, Y.; Lei, J.; Yin, Y.; Ju, H. X. *Chem. Commun.* **2009**, 7161–7163.
(29) Lidstrom, M. E.; Meldrum, D. R. *Nat. Rev. Microbiol.* **2003**, *1*, 158–164.
(30) Krokhin, O. V.; Antonovici, M.; Ens, W.; Wilkins, J. A.; Standing, K. G. *Anal. Chem.* **2006**, *78*, 6645–6650.
(31) Ren, D.; Pipes, G. D.; Liu, D.; Shih, L.-Y.; Nichols, A. C.; Treuheit, M. J.; Brems, D. N.; Bondarenko, P. V. *Anal. Biochem.* **2009**, *392*, 12–21.
(32) Sampathkumar, S.-G.; Jones, M. B.; Yarema, K. J. *Nat. Protoc.* **2006**, *1*, 1840–1851.
(33) Liu, B.; Rotenberg, S. A.; Mirkin, M. V. *Proc. Natl. Acad. Sci. U.S.A.* **2000**, *97*, 9855–9860.
(34) Liu, B.; Rotenberg, S. A.; Mirkin, M. V. *Anal. Chem.* **2002**, *74*, 6340–6348.
(35) Wittstock, G.; Yu, K.; Halsall, H. B.; Ridgway, T. H.; Heineman, W. R. *Anal. Chem.* **1995**, *67*, 3578–3582.
(36) Wittstock, G.; Burchardt, M.; Pust, S. E.; Shen, Y.; Zhao, C. *Angew. Chem., Int. Ed.* **2007**, *46*, 1584–1617.
(37) Mauzeroll, J.; Bard, A. J.; Owhadian, O.; Monks, T. J. *Proc. Natl. Acad. Sci. U.S.A.* **2004**, *101*, 17582–17587.
(38) Yasukawa, T.; Kaya, T.; Matsue, T. *Anal. Chem.* **1999**, *71*, 4637–4641.
(39) Shiku, H.; Shiraishi, T.; Ohya, H.; Matsue, T.; Abe, H.; Hoshi, H.; Kobayashi, M. *Anal. Chem.* **2001**, *73*, 3751–3758.
(40) Hengstenberg, A.; Blöchl, A.; Dietzel, I. D.; Schuhmann, W. *Angew. Chem., Int. Ed.* **2001**, *40*, 905–908.
(41) Isik, S.; Schuhmann, W. *Angew. Chem., Int. Ed.* **2006**, *45*, 7451–7454.
(42) Liebetrau, J. M.; Miller, H. M.; Baur, J. E.; Takacs, S. A.; Anupunpisit, V.; Garris, P. A.; Wipf, D. O. *Anal. Chem.* **2003**, *75*, 563–571.
(43) Kurulugama, R. T.; Wipf, D. O.; Takacs, S. A.; Pongmayteegul, S.; Garris, P. A.; Baur, J. E. *Anal. Chem.* **2005**, *77*, 1111–1117.
(44) Sun, P.; Laforge, F. O.; Abeyweera, T. P.; Rotenberg, S. A.; Carpino, J.; Mirkin, M. V. *Proc. Natl. Acad. Sci. U.S.A.* **2008**, *105*, 443–448.
(45) Takahashi, Y.; Miyamoto, T.; Shiku, H.; Asano, R.; Yasukawa, T.; Kumagai, I.; Matsue, T. *Anal. Chem.* **2009**, *81*, 2785–2790.
(46) Shiku, H.; Matsue, T.; Uchida, I. *Anal. Chem.* **1996**, *68*, 1276–1278.
(47) Shiku, H.; Hara, Y.; Matsue, T.; Uchida, I.; Yamauchi, T. *J. Electroanal. Chem.* **1997**, *438*, 187–190.

Pt wire with a diameter of 50 μm (purity 99.9%, hard) was provided by Alfa Aesar (Ward Hill, MA). Borosilicate glasses with a length of 100 mm, an outer diameter of 1 mm, and an inner diameter of 500 μm were purchased from Sutter Instrument Company (Novata, CA). The quartz capillaries were obtained from Yongnian Optic Fiber Plant (Hebei, China) with an outer diameter of 375 μm and an inner diameter of 100 μm.

Equipment. A P-2000 laser puller from Sutter Instrument Company (Novata, CA) was used for the fabrication of Pt-disk electrodes. The subsequent polishing procedure was accomplished by Narishige EG-400 Microgrinder (Tokyo, Japan), equipped with a standard #5000 grinding wheel composed of diamond stones with radius of 750 nm. Brightfield and fluorescent images were taken by virtue of TE2000-U inverted fluorescence microscope (Nikon, Japan). A two-electrode setup comprising a 0.25 mm Ag/AgCl reference electrode and a Pt-disk microelectrode as working electrode was employed for measurements on a CHI 900 scanning electrochemical microscope (Austin, TX), which was mounted on the horizontal stage of an inverted biological microscope. The reference electrode was verified to be stable during the measurement.

Fabrication of Pt-Disk Tips. Pt wire was cut and inserted into a quartz capillary with the polyimide layer burned off, and then, the quartz capillary was inserted into a borosilicate glass tube. The resulting glass/quartz/wire assembly was placed inside the laser heating chamber with two plastic tubes to hold tightly the sleighs of the puller. A programmatic heating was loaded to ensure the optimal sealing of the Pt wire first. After the plastic tubes were removed, a second program was employed to produce two Pt wires sealed tightly in the capillary. After electrical contact and sealing the opening end, another end with the Pt-disk tip was polished in a drop of water by slowly lowering down the tip holder onto a rotary polishing plate using a manual micropositioning element until the desired active size (1 μm radius) was obtained, which was monitored by performing cyclic voltammetry in 0.1 M KCl containing 1.0 mM $K_3Fe(CN)_6$. As shown in Figure S-1C in Supporting Information, the active radius of the obtained tip was calculated from the steady-state current to be 1.0 μm. The RG value, the ratio of the overall radius to the radius of the conductor, of the Pt-disk tip was estimated from the front view to be 10 (Figure S-1B in Supporting Information), and the SECM approach curve further showed that the tip was suitable for quantitative experiments (Figure S-1D in Supporting Information).

Cell Culture. BGC cells were kindly provided by Affiliated Zhongda Hospital of Southeast University, Nanjing, China, and cultured in a flask in RPMI 1640 medium (GIBCO) supplemented with 10% fetal calf serum (FCS, Sigma), penicillin (100 μg mL^{-1}), and streptomycin (100 μg mL^{-1}) at 37 °C in a humidified atmosphere containing 5% CO_2. At the logarithmic growth phase, the cells were trypsinized and washed twice with sterile 0.01 M, pH 7.4 PBS by centrifugation at 1000 rpm for 6 min. The sediment was then resuspended in culture medium.

Micropatterning of BGC Cells. PDMS membrane was prepared by coating a mixture of silicone elastomer and curing agent on a glass sheet. The thickness of the PDMS membrane was estimated to be 120 μm by optical microscopy. An array of micrometer-sized holes was then formed on the PDMS sheet by simply drilling with a syringe needle. Afterward, the PDMS sheet was covered on a 35 mm dish to form an array of microwells, and BGC cells in culture medium (10^6 cells mL^{-1}, 100 μL) were added into an individual microwell. After incubation for 4 h to allow the adhesion of cells to the dish, the excess nonadherent cells were removed by washing with RPMI-1640. After further incubation in cell-free culture medium for 1 day, 5 μL of 3% BSA was added into the microwell to block the located BGC cells for 10 min, and then, 100 μL of 1 μg mL^{-1} HRP-lectin was added for the recognition of membrane glycan by incubation for another 45 min. For the binding of HRP-ConA to mannose on cell membrane, 1 mM Ca^{2+} and Mn^{2+} should be added to HRP-ConA solution. PDMS membrane was finally peeled off from the dish, and the adherent cells were used for SECM measurement at a single-cell level. The cell cycle period and the interphase of BGC-823 cells are 41 and 40 h, respectively. After incubation for 24 h, the average height of BGC cells was about 11 μm, as determined by optical microscopy, and the micrograph showed that most of the cells had similar size, and their shape was in interphase (Figure S-2 in Supporting Information), in which the cell height variation (<1 μm) was regarded as negligible.[48]

SECM Procedure. First, the 2 μm Pt tip was applied a potential of −0.5 V for oxygen reduction, approached to the Petri dish bottom, and stopped at 70% of the steady-state current, which corresponded to a 2 μm tip−substrate separation distance calculated from the approach curve in PBS (Figure S-1 in Supporting Information). Afterward, the tip was retracted by 13 μm to obtain a 15 μm separation between the tip and Petri dish bottom. Thus, the tip−cell separation distance was about 4 μm. Then, SG/TC mode was employed to perform the single-cell SECM experiments using PBS (pH 7.4) containing 1.0 mM H_2O_2 and 1.0 mM FMA as the electrolyte. The potential of working electrode was set at 0.05 V vs Ag/AgCl for the reduction of FMA^+ with a scan rate of 10 μm s^{-1}. The peak current at the center of the cell (i_p) was used for optimizing the experiment parameters. The center of the cell was the point corresponding to the maximum current value, which was defined in Figure S-3 in Supporting Information.

Flow Cytometric Analysis. The adherent BGC cells were collected and separated from the medium by centrifugation at 1000 rpm at room temperature for 6 min. Subsequently, the cells were washed with sterile, cold, pH 7.4 PBS and resuspended in PBS. The cell concentration was determined. Then, 50 μL of a 1×10^7 cells mL^{-1} cell suspension and 445 μL of pH 7.4 PBS were mixed with 5 μL of 1 mg mL^{-1} FITC-labeled lectins (DBA, ConA, PNA, and WGA) and incubated at room temperature for 30 min, respectively. The cells were collected by centrifugation at 1000 rpm for 6 min, washed twice with 200 μL of cold PBS, resuspended in 500 μL of PBS, and assayed by flow cytometry. Unlabeled cells were used for estimation of autofluorescence.

RESULTS AND DISCUSSION

Pattern of Adherent BGC Cells. For single-cell analysis, the efficient control of cell location and labeling of target cells with minimum nonspecific adsorption of the substrate require the

(48) Jeanes, A.; Smutny, M.; Leerberg, J. M.; Yap, A. S. *J. Mol. Histol.* **2009**, *40*, 395–405.

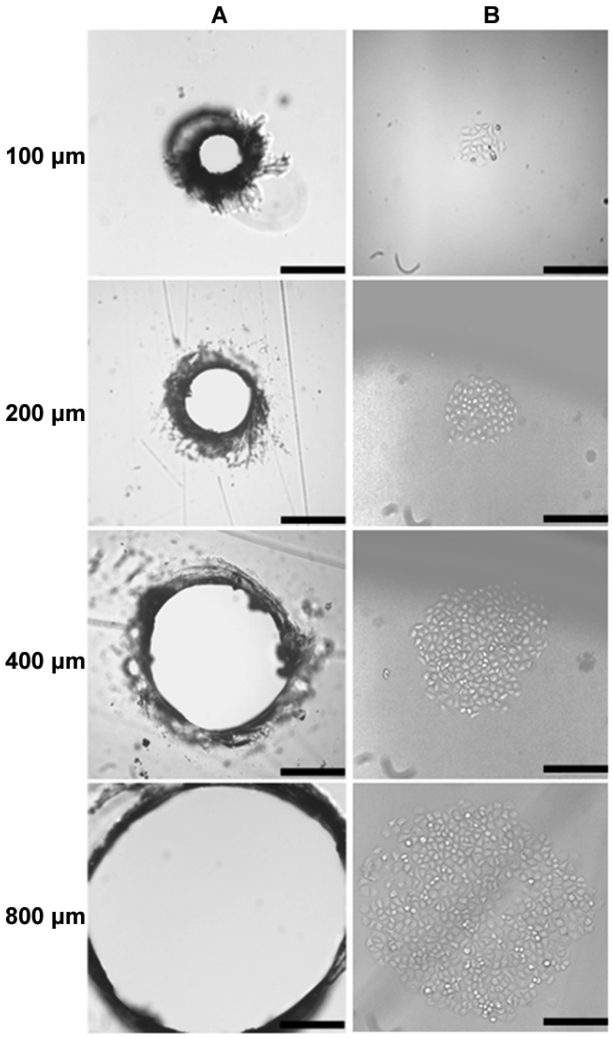

Figure 2. Optical micrographs of (A) PDMS membranes with microwells of 100, 200, 400, and 800 μm, and (B) cell patterns formed after further incubation in the cell-free culture medium for 1 day. Scale bar: 200 μm.

convenient patterning of cells.[49] Microcontact printing has been well-established for the patterning of living cells using PDMS coupled with photolithography or laser etching technique.[50−52] This work simply prepared the PDMS microwells by drilling the PDMS sheet with syringe needles and then covering the PDMS sheet on a dish. The optical microscopic images of four PDMS microwells showed well shape with diameters of 100, 200, 400, and 800 μm (Figure 2A). These well-shaped microwells on the flexible membrane allowed the convenient patterning of adherent BGC cells. After the cell suspension (10^6 cells mL^{-1}) was gently added into the PDMS microwells, the cells quickly adhered to the Petri dish surface. During the further incubation in cell-free culture medium, adherent BGC cells began to spread and grow within the restricted microwells, which could be observed from the optical micrographs of the patterned cells (Figure 2B). The smallest cell pattern with the diameter of 100 μm contained only about 15 BGC cells. In fact, by decreasing the concentration of cell suspension and the subsequent incubation time, a cell pattern with only one BGC cell could be obtained via the same procedure. The adherent BGC cell patterns were stable for at least 2 days under the cultivation conditions. The uniform cell pattern enabled the control and monitoring of the recognition of membrane glycans on localized living cells with a small amount of HRP-lectins.

Table 1. Glycan-Binding Specificities of the Lectins

lectins	origin	binding specificity
WGA	*Triticum unlgari*	(Neu5Ac[a]) (Gal[b] β4GlcNAc[c])1-3,4 (GlcNAc β4GlcNAc)1-3,4
ConA	*Canavalia ensiformis*	terminal α Man[d], Man α3[Man α6] Man
PNA	*Arachis hypogaea*	Gal β(1,3)GalNAc[e], terminal βGal
DBA	*Dolichos biflorus*	GalNAc α1,3 GalNAc/Gal

[a] Neu5Ac: *N*-acetylneuraminic acid. [b] Gal: galactose. [c] GlcNAc: *N*-acetylglucosamine. [d] Man: mannose. [e] GalNAc: *N*-acetylgalactosamine.

Specific Recognition of Cell-Surface Glycans with HRP-Lectins. Lectin-based technology has been applied to detect selectively cell-surface glycoconjugate and to identify glycoproteins in gels and on protein blots due to the highly specific binding affinity of lectins to carbohydrates.[53] The binding specificities of the lectins used were listed in Table 1. Using WGA, an *N*-acetyl-D-glucosamine (GlcNAc)/*N*-acetyl-D-neuraminic acid-specific lectin,[54] as the model, the fluorescent image of BSA-blocked BGC cells after incubation with FITC-labeled WGA was shown in Figure 3A. Green fluorescence emitted from FITC was clearly observed for the whole cell pattern, which demonstrated the successful binding of FITC-WGA to cell-surface glycans. Nevertheless, initial incubation of BSA-blocked BGC tumor cells with WGA led to occupation of the target glycan sites, which prevented subsequent binding of the FITC-WGA; thus, the fluorescence emission could hardly be observed (Figure 3B). This result demonstrated that the micropatterning method achieved the efficient recognition of cell-surface glycans toward lectins and also prevented the non-specific adsorption of proteins around the cells.

Optimization of HRP-Lectin Concentration and Recognition Time. The fluorescent microscopy allows adherent cells to be measured in situ, but it is not suitable for quantitative analysis due to photobleaching and autofluorescence of the cell itself.[45] Taking the advantages of SG/TC SECM measurement, it is possible to monitor membrane glycan expression on living cells with the help of enzyme-tagged lectins, owing to the fast detection of diffusion current of electroactive enzymatic product by SECM. Considering the low expression of some glycan motifs on cell surface, HRP, a highly active enzyme, was chosen to tag lectin for glycan imaging at a single-cell level. The HRP tagged on cell surface upon the recognition process could catalyze the oxidation of FMA by H_2O_2 to yield the oxidized mediator FMA^+. The FMA^+ diffused to the tip of the Pt-disk probe to produce the

(49) Rosenthala, A.; Macdonaldc, A.; Voldmanb, J. *Biomaterials* **2007**, *28*, 3208–3216.
(50) Xia, Y.; Kim, E.; Zhao, X.-M.; Rogers, J. A.; Prentiss, M.; Whitesides, G. M. *Science* **1996**, *273*, 347–349.
(51) Kane, R. S.; Takayama, S.; Ostuni, E.; Ingber, D. E.; Whitesides, G. M. *Biomaterials* **1999**, *20*, 2363–2376.
(52) Amirpour, M. L.; Chosh, P.; Lackowski, W. M.; Crooks, R. M.; Pishko, M. V. *Anal. Chem.* **2001**, *73*, 1560–1566.
(53) Zhelev, Z.; Ohba, H.; Bakalova, R.; Jose, R.; Fukuoka, S.; Nagase, T.; Ishikawa, M.; Baba, Y. *Chem. Commun.* **2005**, 1980–1982.
(54) Loris, R.; De Greve, H.; Dao-Thi, M. H.; Messens, J.; Imberty, A.; Wyns, L. *J. Mol. Biol.* **2000**, *301*, 987–1002.

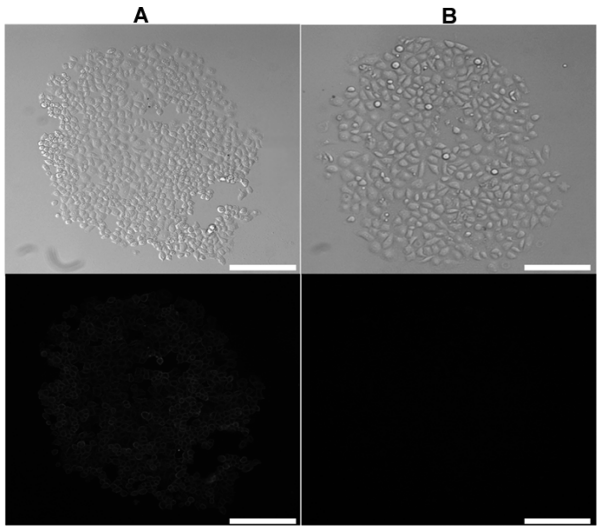

Figure 3. Optical and fluorescent images of BSA-blocked BGC cell patterns after incubation with (A) 0.5 μM FITC-WGA for 45 min and (B) 0.5 μM WGA for 15 min and then 0.5 μM FITC-WGA for 45 min. Scale bar: 200 μm.

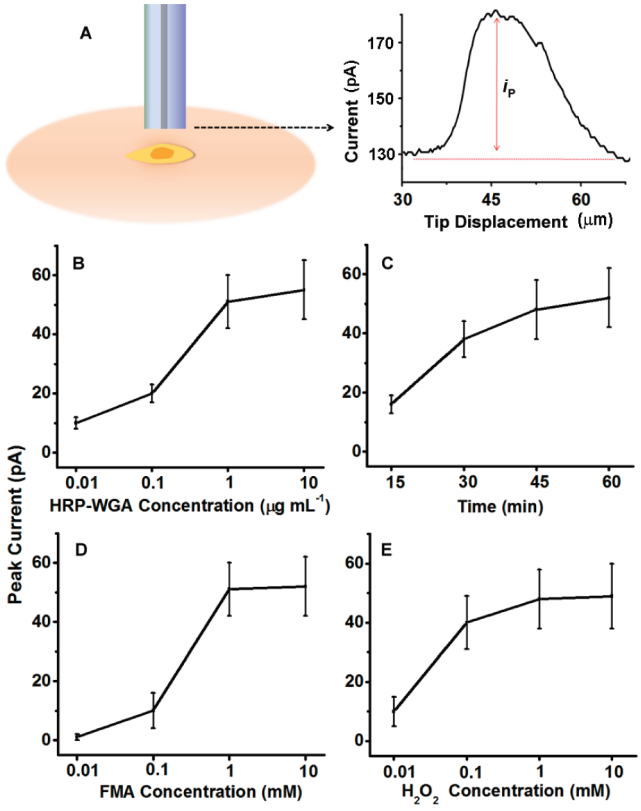

Figure 4. (A) SECM one-line scan curve obtained above single BGC cell labeled with HRP-WGA, and dependence of peak current on (B) HRP-WGA concentration, (C) binding time, (D) FMA concentration, and (E) H_2O_2 concentration (n = 8). When one parameter changes, the others are under their optimal conditions.

reduction current, which was the only electrode reaction at the tip, for imaging the expression level of membrane glycans (Figure 4A). In addition, the FMA generated at the tip diffused back to the cell surface, where it was reoxidized through the enzyme reaction again. This redox cycle generated additional reduction current for enhancing the response. The peak response (i_P) recorded at the center of the cell depended on the amount of HRP-lectin bound to cell-surface glycans, which was related to the concentration of HRP-lectin used for the recognition step and the recognition time.

With the increasing HRP-WGA concentration from 0.01 to 1 μg mL^{-1}, the i_P value increased from 10 to about 50 pA (Figure 4B). The further increase of HRP-WGA concentration did not obviously change the response, indicating most of the target cell-surface glycan sites on adherent BGC cell were already bound sufficiently. The large error bars (n = 8) observed at lectin concentrations higher than 1 μg mL^{-1} might result from the heterogeneity among single cells. To in situ exhibit the exact glycan expression on adherent BGC cells, 1 μg mL^{-1} was chosen as the optimal HRP-lectin concentration, at which the peak current gradually increased with the increasing incubation time and tended to a steady value after 45 min (Figure 4C), indicating the saturated binding of corresponding BGC membrane glycans. Therefore, an incubation time of 45 min was chosen for the following experiments.

Optimization of Detection Condition. The performance of enzyme-catalyzed SECM imaging was related to the concentration of FMA and H_2O_2 in the measuring system. The peak current recorded in pH 7.4 PBS increased with the increasing concentrations of both FMA and H_2O_2 from 0.01 to 1.0 mM and then maintained the maximum value at higher concentrations (Figure 4D,E), which assured that the enzymatic reaction rate was dependent on the amount of the recognized HRP. Therefore, both optimal FMA and H_2O_2 concentrations for enzyme-catalyzed SECM detection were 1.0 mM. A trypan blue experiment indicated that the cells could keep good viability in this solution during the SECM measurement (Figure S-4 in Supporting Information). Although the system might be complicated, the profile was almost independent of the concentration of H_2O_2 at higher than 1.0 mM, and the response was only controlled by the reaction between HRP and FMA.[46] Since the reaction between HRP and FMA did not change solution pH and the SECM measurements were performed in pH 7.4 PBS, the effect of local pH change resulting from the reduction of H_2O_2 by the reduced HRP on the response could be neglected.[46]

SECM Imaging of WGA-Specific Membrane Glycans on a Single Adherent BGC Cell. Under the optimal conditions, the single-cell SECM images of glycans on BGC cell surface with and without HRP-WGA labeling were showed in Figure 5. The current response of the HRP-labeled BGC cell was considerably larger than that of nonlabeled cell, indicating that the binding of HRP-WGA to cell-surface glycan motifs could be successfully visualized via SECM. The baseline tip current for WGA-labeled cells was remarkably higher than that for nonlabeled cells. This might be attributed to the diffusion of FMA^+ produced from abundant WGA-recognized sites on the BGC cell surface to the bulk solution. A slight response was observed for a nonlabeled cell in Figure 5A, which was due to the fact that mammalian cells naturally express endogenous peroxidase.[33,55] This response for

(55) Zhang, X.; Sun, F.; Peng, X.; Jin, W. *Anal. Chem.* **2007**, *79*, 1256–1261.

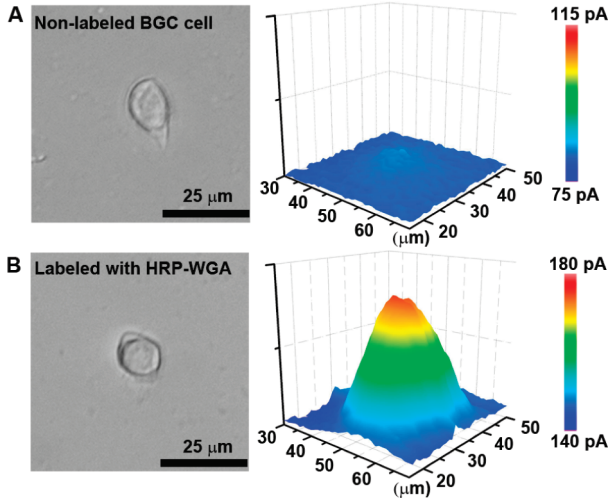

Figure 5. Optical and SECM images of (A) a nonlabeled BGC cell and (B) a HRP-WGA labeled BGC cell in PBS containing 1.0 mM FMA and H_2O_2.

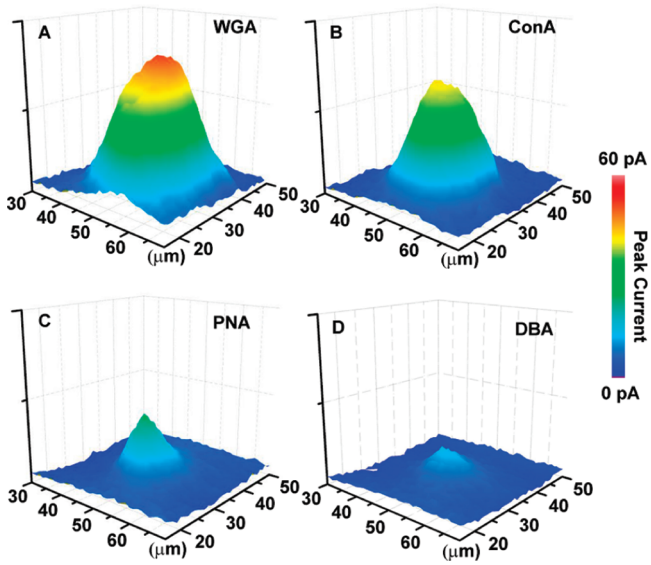

Figure 6. Single-cell SECM images in situ recorded in PBS containing FMA and H_2O_2 for BGC cells after incubation with (A) HRP-WGA, (B) HRP-ConA, (C) HRP-PNA, and (D) HRP-DBA. For facile comparison, the baselines of tip current are corrected as 0.

nonlabeled BGC cells was 3.2 ± 2.5 pA (n = 8), which was considered as the background signal in subsequent statistic analysis.

In Situ Electrochemical Imaging of Four Types of Membrane Glycan Motifs. Figure 6 shows the single-cell SECM images for BGC cells in PBS containing FMA and H_2O_2 after incubation with HRP-WGA, HRP-ConA, HRP-PNA, and HRP-DBA, respectively. For facile comparison, the baselines of tip current are corrected as 0. Although SECM measurements were performed at the same lectin concentration and binding time, the difference in current responses among four lectins was clearly observed. Since the current response depended on the amount of HRP-lectin specifically bound to cells, the observed difference reflected the different expression levels of distinct membrane glycan motifs. The

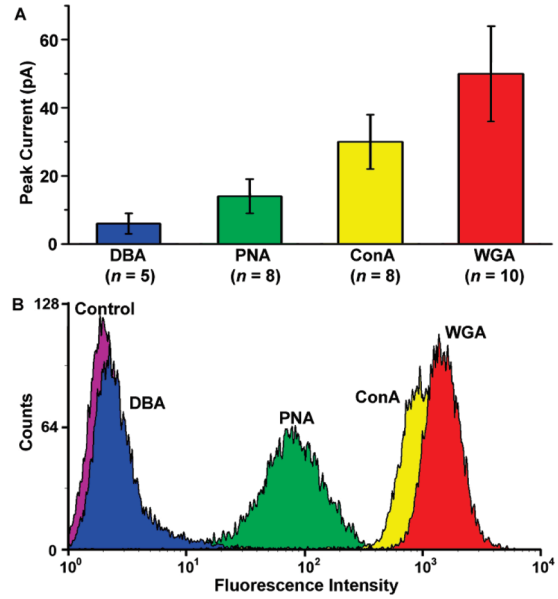

Figure 7. Relative expression levels of four glycan motifs on an adherent single BGC cell surface measured by (A) SECM in SG/TC mode after background subtraction and (B) flow cytometric fluorescence profiles after treated with FITC-lectins.

SECM images indicated that the BGC cell surface expressed high abundance of WGA-specific glycans, moderate abundance of ConA-specific glycans, and low abundance of PNA- and DBA-specific glycans.

SECM could not only be used to distinguish visually the glycan expression levels of single living cells but also provide the qualitative comparison of the expression level.[45] After subtracting the background signal of nonlabeled cells, the peak currents for BGC cells incubated with HRP-WGA, HRP-ConA, HRP-PNA, and HRP-DBA were 50 ± 14 pA (n = 10), 30 ± 8 pA (n = 8), 14 ± 5 pA (n = 8), and 6 ± 3 pA (n = 5) (Figure 7A), respectively. Statistically significant differences were found in the responses for four types of glycan motifs as follows: DBA- < PNA- < ConA- < WGA-specific glycans (p < 0.006, DBA- and PNA-specific; p < 0.002, PNA- and ConA-specific; p < 0.003, ConA- and WGA-specific). The same order of cell-surface glycan expression levels was also found in measurements by flow cytometry (Figure 7B). The identical results indicated that SECM measurement could provide a reliable estimation of the cell-surface glycan expression levels.

CONCLUSIONS

This work proposed an efficient method for in situ electrochemically imaging of membrane glycan motifs on adherent single cells by SECM. By integrating SG/TC SECM, micropatterning, and specific recognition between biomolecules, the relative expression levels of different membrane glycans on localized adherent BGC cells were measured without peeling the cells from the culture dish. The SECM results demonstrated that the expression levels for cell-surface glycans were statistically distinguishable in the following descending order: WGA-, ConA-, PNA-, and DBA-specific glycans, which was consistent with the flow cytometric assay. Due to the noninvasive and continuous nature of SECM, this technique could be expanded for real-time monitoring of the dynamic changes in the

glycosylation status on cell surface, particularly carcinoma cell surfaces. Although the proposed method could not provide molecular details, it allowed investigation into the most biologically relevant surface-accessible glycan motifs with the addition of more glycan/lectin (antibody) interaction pairs to the repertoire. Thus, this work affords a promising protocol for research of cell biology related to cell-surface carbohydrate expression.

ACKNOWLEDGMENT

We gratefully acknowledge the National Science Funds for Creative Research Groups (20821063), the Major Research Plan (90713015) and General Program (20875044) from the National Natural Science Foundation of China, and National Basic Research Program of China (2010CB732400).

SUPPORTING INFORMATION AVAILABLE

Additional information as noted in text. This material is available free of charge via the Internet at http://pubs.acs.org.

Received for review February 8, 2010. Accepted July 22, 2010.

AC101688P